Cellular/Molecular

Loss of hnRNP K Impairs Synaptic Plasticity in Hippocampal Neurons

Alessandra Folci,[1] Lisa Mapelli,[1,2,3] Jenny Sassone,[4] Francesca Prestori,[2] Egidio D'Angelo,[2,3] Silvia Bassani,[1]* and Maria Passafaro[1]*

[1]CNR Institute of Neuroscience, Department of Medical Biotechnology and Translational Medicine (BIOMETRA), University of Milan, Milan 20129, Italy, [2]Department of Brain and Behavioral Sciences, Neurophysiology Unit, University of Pavia, Pavia 27100, Italy, [3]Brain Connectivity Center, C. Mondino National Neurological Institute, Pavia 27100, Italy, and [4]IRCCS Istituto Auxologico Italiano, Department of Neurology and Laboratory of Neuroscience, Milan 20095, Italy

Heterogeneous nuclear ribonucleoprotein K (hnRNP K) is an RNA-binding protein implicated in RNA metabolism. Here, we investigated the role of hnRNP K in synapse function. We demonstrated that hnRNP K regulates dendritic spine density and long-term potentiation (LTP) in cultured hippocampal neurons from embryonic rats. LTP requires the extracellular signal-regulated kinase (ERK)1/2-mediated phosphorylation and cytoplasmic accumulation of hnRNP K. Moreover, hnRNP K knockdown prevents ERK cascade activation and GluA1-S845 phosphorylation and surface delivery, which are essential steps for LTP. These findings establish hnRNP K as a new critical regulator of synaptic transmission and plasticity in hippocampal neurons.

Key words: **dendritic spines; hnRNP K; LTP; neurons; synapse**

Introduction

Heterogeneous nuclear ribonucleoprotein K (hnRNP K) is an RNA-binding protein (RBP) involved in RNA metabolism (Glisovic et al., 2008). hnRNP K is a substrate of various kinases, and both its localization and activity are modulated by phosphorylation (Habelhah et al., 2001). hnRNP K post-transcriptionally regulates multiple cytoskeletal genes, including Actin Related Protein 2 (Arp2), thereby promoting axon outgrowth in *Xenopus laevis* (Liu et al., 2008; Liu and Szaro, 2011). Furthermore, hnRNP K interacts with Wiskott–Aldrich syndrome protein (N-WASP), indicating a role in the regulation of actin dynamics (Yoo et al., 2006). hnRNP K also interacts with Abelson-interacting protein 1, thereby regulating dendritic arborization in neurons (Proepper et al., 2011). In the rat brain, hnRNP K is widely expressed during development, and its expression is maintained throughout adulthood in the neocortex, the hippocampus, and the cerebellum (Proepper et al., 2011). Here, we investigated the synaptic role of hnRNP K in hippocampal neurons. We demonstrated that hnRNP K regulates the density and molecular composition of dendritic spines. Moreover, hnRNP K is required for extracellular signal-regulated kinase (ERK) cascade activation and long-term potentiation (LTP) in hippocampal neurons.

Received Jan. 22, 2014; revised May 12, 2014; accepted May 30, 2014.

Author contributions: A.F., S.B., and M.P. designed research; A.F., L.M., J.S., F.P., and S.B. performed research; A.F., E.D., S.B., and M.P. analyzed data; A.F., J.S., S.B., and M.P. wrote the paper.

This work was supported by Telethon Italy (TDMP00607/TELU, M.P.). We thank Dr. Ronai Z. for the kind gifts of HA-hnRNP K WT and HA-hnRNP K S284A/S353A and Dr. Valentina Cea for technical support.

The authors declare no competing financial interests.

*S.B. and M.P. contributed equally to this work.

Correspondence should be addressed to either Silvia Bassani or Maria Passafaro, CNR Institute of Neuroscience, Department of Medical Biotechnology and Translational Medicine (BIOMETRA), University of Milan, 32 Via Vanvitelli, Milan 20129, Italy, E-mail: s.bassani@in.cnr.it or m.passafaro@in.cnr.it.

DOI:10.1523/JNEUROSCI.0303-14.2014

 0270-6474/14/349088-08$15.00/0

Materials and Methods

Cell culture and transfection. All experiments were performed on dissociated hippocampal neurons prepared from rat embryos of either sex at a gestational age of 18 d and transfected at 12 d *in vitro* (DIV) using the calcium phosphate method as previously described (Bassani et al., 2012). The neurons were used at 18 DIV.

cDNA constructs. hnRNP K siRNA (Lynch et al., 2005) and scrambled siRNA (scrambled) sequences were cloned into the vectors pLL3.7 and pLVTHM. HA-hnRNP K WT and HA-hnRNP K S284A/S353A were a kind gift from Dr. Ronai Z. (Habelhah et al., 2001).

Lentiviral infection. Hippocampal neurons were infected at 8 DIV with siRNA or scrambled as previously described (Bassani et al., 2012) and were used at 18 DIV.

Immunostaining. Hippocampal neurons were stained and analyzed as previously described (Bassani et al., 2012). Images were acquired with an LSM 510 Meta confocal microscope (Carl Zeiss; gift from F. Monzino).

Protein extraction and fractionation. Total homogenates and nucleus/cytoplasm fractionation were performed as previously described (Laury-Kleintop et al., 2005). The crude synaptosomal fraction (P2) was obtained as previously described (Proepper et al., 2011).

Biotinylation assay. The biotinylation assay was performed as previously described (Ehlers, 2000).

Real-time PCR. Cell lysis, RNA extraction, genomic DNA removal, reverse transcription, and real-time PCR were performed with a TaqMan Gene Expression Cells-to-CT Kit (Life Technologies). cDNAs were amplified by real-time PCR using the TaqMan Gene Expression Master Mix and the TaqMan Gene Expression Assays Rn00470532_g1 (hnRNP K) and Rn99999916_s1 (GAPDH).

Antibodies. The following antibodies and dilutions were used: rabbit antibodies against hnRNP K [1:100 for immunofluorescence (IF) and 1:5000 for Western blot (WB); MBL], vesicular glutamate transporter 1 (VGLUT1; 1:800; Synaptic Systems), GluA1 (1:2000; Millipore),

GAPDH (1:1000; Santa Cruz Biotechnology), pGluA1-S845 (1:1000; Cell Signaling Technology), vesicular GABA transporter (VGAT; 1:800; Synaptic Systems), phnRNP K-S284 (1:500; Sigma-Aldrich), and mitogen-activated protein kinase kinase 1/2 (MEK1/2; 1:500; Santa Cruz Biotechnology); mouse antibodies against PSD-95 (1:200 for IF and 1:10,000 for WB; NeuroMab), GluA2 (1:200; Millipore), and SP1 (1:1000; Millipore); and a goat antibody against pMEK1/2 (1:500; Santa Cruz Biotechnology).

Electrophysiology. Whole-cell patch-clamp recordings were performed as previously described (Bassani et al., 2012). The decay of the miniature EPSCs (mEPSCs) was fitted using a bi-exponential equation. For chemical LTP (cLTP) experiments, a glycine solution was used as previously described (Lu et al., 2001). After 10 min of stable recording of mEPSCs, the cLTP solution was perfused for 3 min. mEPSCs were then recorded for 40 min after induction or used for WB or IF as described.

Calcium imaging. To measure intracellular calcium concentration ($[Ca^{2+}]_i$) changes, neurons were loaded with an intracellular solution containing 200 μM Oregon Green BAPTA-1. Dendritic fluorescence (F) was monitored for 5–7 min before, 10 min after, and during the 3 min of glycine perfusion (Gall et al., 2005). For each condition, multiple regions of interest (ROIs) in two to three dendrites of each neuron were considered for analysis. The ROI fluorescence intensity (F) was normalized against the background fluorescence (Fb), and F-Fb was then analyzed.

Statistics. Data are expressed as the mean ± SEM. Statistical significance was assessed using an unpaired Student's *t* test (two means) or one-way ANOVA with an appropriate *post hoc* test (more than two means). Each experiment was repeated three times using neurons from three independent preparations. At least seven neurons per condition from each preparation were analyzed for IF.

Results

hnRNP K knockdown affects synaptic density and transmission

In hippocampal neurons, hnRNP K was detected in the dendritic spines and colocalized with the presynaptic protein VGLUT1 and the postsynaptic scaffolding protein PSD-95 (Fig. 1*A*).

To explore the role of hnRNP K in neurons, we knocked down hnRNP K using a specific siRNA (Lynch et al., 2005) and determined that hnRNP K silencing reduced the dendritic length and branching and the spine density (Fig. 1*B*,*C*), while the spine shape remained unchanged (data not shown). These effects were prevented by the coexpression of an siRNA-resistant hnRNP K (rescue; Fig. 1*B*,*C*). We next examined the effect of hnRNP K knockdown on synaptic protein expression. GluA2 and PSD-95 expression were significantly reduced following hnRNP K silencing, whereas VGAT, VGLUT, GluA1, synapsin, and synaptophysin were unchanged (Fig. 1*D*; data not shown). Coexpression of the siRNA-resistant hnRNP K normalized GluA2 and PSD-95 protein levels (Fig. 1*D*).

We next investigated whether hnRNP K modulates excitatory synaptic transmission by recording mEPSCs in hnRNP K-silenced hippocampal neurons. hnRNP K silencing did not change the current peak amplitude but specifically decreased the mEPSC frequency. The currents of silenced neurons were also characterized by slower decay kinetics compared with those of scrambled and rescued neurons (Fig. 1*E*). These results indicate that hnRNP K regulates the density and molecular composition of dendritic spines and spontaneous excitatory transmission.

cLTP induces the expression, phosphorylation, and cytoplasmic accumulation of hnRNP K

Because the levels of many RBPs increase with synaptic activity (Zhang et al., 2012), we tested the hypothesis that cLTP modifies the levels and distribution of hnRNP K. Upon cLTP induction, we observed a transient increase in hnRNP K mRNA after 25 min (Fig. 2*A*) and a sustained increase in hnRNP K protein from 25 to 75 min (Fig. 2*B*).

Treatment with 5,6-dichloro-1-β-D-ribofuranosylbenzimidazole (DRB) and cycloheximide (CHX), which inhibit transcription and protein synthesis, respectively, prevented the effects of cLTP on hnRNP K expression (Fig. 2*C*,*D*). Furthermore, 25 min after cLTP induction, the phosphorylation of S284 of hnRNP K increased (Fig. 2*E*). S284 is a target of ERK1/2 (Habelhah et al., 2001); thus, we treated neurons with the ERK1/2 inhibitor U0126 and observed that U0126 prevented hnRNP K phosphorylation (Fig. 2*F*). Because the subcellular distribution and activity of hnRNP K can be modified by phosphorylation (Habelhah et al., 2001), we performed subcellular fractionation experiments and observed that cLTP increased the level of hnRNP K in the cytoplasm (Fig. 2*G*), while the hnRNP K levels in the crude synaptosomal fraction (P2) remained unchanged (Fig. 2*H*). Overall, our results indicate that cLTP increases the expression, ERK1/2-mediated phosphorylation, and cytoplasmic recruitment of hnRNP K, strongly supporting its involvement in LTP processes.

hnRNP K knockdown precludes cLTP in hippocampal neurons

We investigated cLTP in hippocampal neurons expressing hnRNP K siRNA or the scrambled sequence. In agreement with a previous report (Kim et al., 2007), cLTP increased the PSD-95 cluster size and PSD-95/VGLUT1 colocalization in control neurons (Fig. 3*A*). Notably, the hnRNP K-silenced neurons displayed a reduced PSD-95 cluster size and PSD-95/VGLUT1 area of colocalization under basal conditions, and both parameters decreased following cLTP (Fig. 3*A*).

cLTP induction increased the amplitude and frequency of mEPSCs and decreased the coefficient of variation in control neurons (Fig. 3*B*; data not shown). Conversely, cLTP induction in hnRNP K-silenced neurons decreased the amplitude of mEPSCs without affecting the frequency or coefficient of variation (Fig. 3*B*; data not shown). These effects were rescued by coexpressing hnRNP K siRNA with WT hnRNP K.

Although the hnRNP K mutant (S284A/S353A), which cannot be phosphorylated by ERK1/2 (Habelhah et al., 2001), did not rescue LTP, the decrease in mEPSC amplitude observed in silenced neurons after glycine treatment was not observed (Fig. 3*B*; data not shown).

These data demonstrate that hnRNP K expression and phosphorylation are necessary for cLTP induction in hippocampal neurons. Notably, the S284A/S353A mutant was able to rescue the effects on dendritic spine density and mEPSC frequency (Fig. 3*C*,*D*), which indicates that hnRNP K phosphorylation is not required for spine density or basal excitatory transmission.

Next, we assessed whether hnRNP K silencing modifies LTP by affecting NMDAR currents. The NMDAR current amplitude, NMDA/AMPA current ratio, and NMDAR current decay kinetics were similar between scrambled and silenced neurons (Fig. 3*E*).

As changes in the calcium threshold can underpin an LTP/LTD switch (Cummings et al., 1996), we measured the increase in intracellular calcium in dendrites, normalized for the number of spines, during glycine perfusion. No differences were observed between scrambled and siRNA-expressing neurons (Fig. 3*F*). These results suggest that hnRNP K silencing prevents cLTP through a mechanism that is independent of NMDAR and calcium influx.

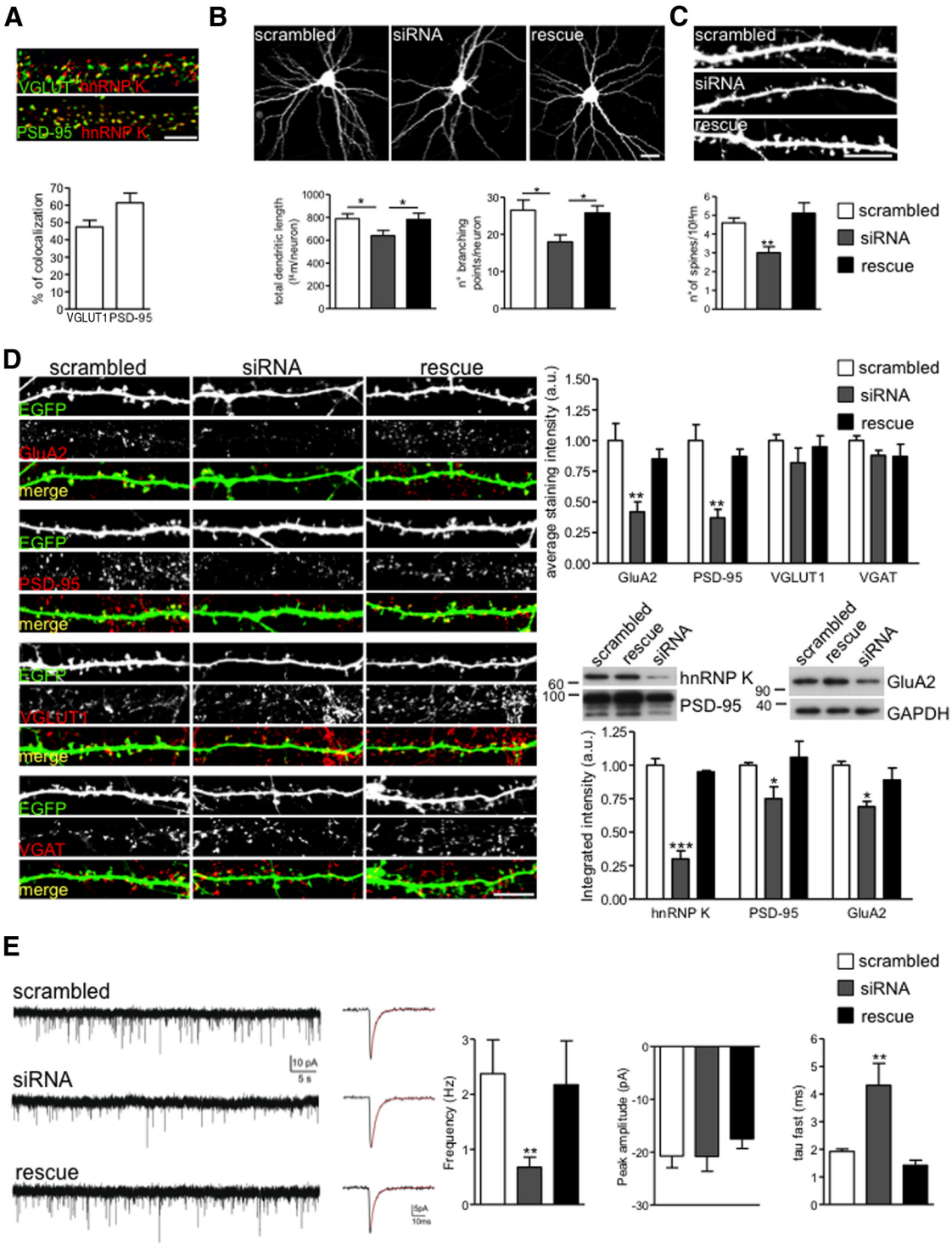

Figure 1. hnRNP K knockdown impairs dendritic spine density and synaptic function. ***A***, Labeling of endogenous hnRNP K and PSD-95 or VGLUT1 in neurons. Scale bar, 5 μm. The histogram represents the percentage of hnRNP K-positive puncta that colocalized with VGLUT1 (47.41 $\pm$ 3.92%) and PSD-95 (61.38 $\pm$ 5.64%). ***B***, Analysis of dendrites in neurons transfected with scrambled or siRNA or rescue. Scale bar, 20 μm. Silenced neurons exhibited reduced dendritic length and branching compared with scrambled and rescue neurons (length μm/neuron: scrambled 787.89 $\pm$ 44, siRNA 638.63 $\pm$ 46.25, rescue 783.08 $\pm$ 61.81; number of branching points per neuron: scrambled 26.55 $\pm$ 2.71, siRNA 18 $\pm$ 1.87, rescue 25.81 $\pm$ 1.9; ANOVA and Bonferroni *post hoc* test, $^{*}p < 0.05$). ***C***, Analysis of dendritic spine density in neurons transfected with scrambled or siRNA or rescue constructs. Scale bar, 10 μm. In silenced neurons, the dendritic spine density was reduced compared with controls (spines/10 μm: scrambled 4.59 $\pm$ 0.26, siRNA 3.01 $\pm$ 0.32; ANOVA and Bonferroni *post hoc* test, $^{**}p < 0.01$). Rescued neurons exhibited normal spine density. ***D***, Analysis of synaptic markers evaluated by IF (transfected neurons) and WB (infected neurons). Scale bar, 10 μm. The staining intensity was measured along the dendrites of the transfected neurons. Compared with scrambled neurons, the staining intensity for GluA2 and PSD-95 was significantly lower in silenced neurons (GluA2: 0.42 $\pm$ 0.08 vs 1 $\pm$ 0.14, $^{**}p < 0.01$; PSD-95: 0.37 $\pm$ 0.07 vs 1 $\pm$ 0.13 $^{**}p < 0.01$; ANOVA and Bonferroni *post hoc* test, values normalized to scrambled), while the staining intensity of VGLUT1 and VGAT was unchanged. Rescued neurons exhibited normal levels of GluA2 and PSD-95. The decrease in GluA2 and PSD-95 staining was reconfirmed by WB analysis of infected neurons ($^{***}p < 0.001$; $^{*}p < 0.05$). ***E***, Representative mEPSC recordings (left) and average traces of 50 mEPSCs (right) from neurons transfected with scrambled, siRNA, or rescue. siRNA neurons exhibited a significant decrease in the frequency (scrambled: 2.4 $\pm$ 0.6 Hz, siRNA: 0.7 $\pm$ 0.2 Hz, $^{**}p < 0.01$) and slower decay kinetics compared with the scrambled and rescued neurons (tau fast of 4.32 $\pm$ 0.79 ms vs 1.92 $\pm$ 0.09 and 1.42 $\pm$ 0.18 ms, respectively; $^{**}p < 0.01$ siRNA vs both scrambled and rescue). The curve in red represents the fitting of the decay phase.

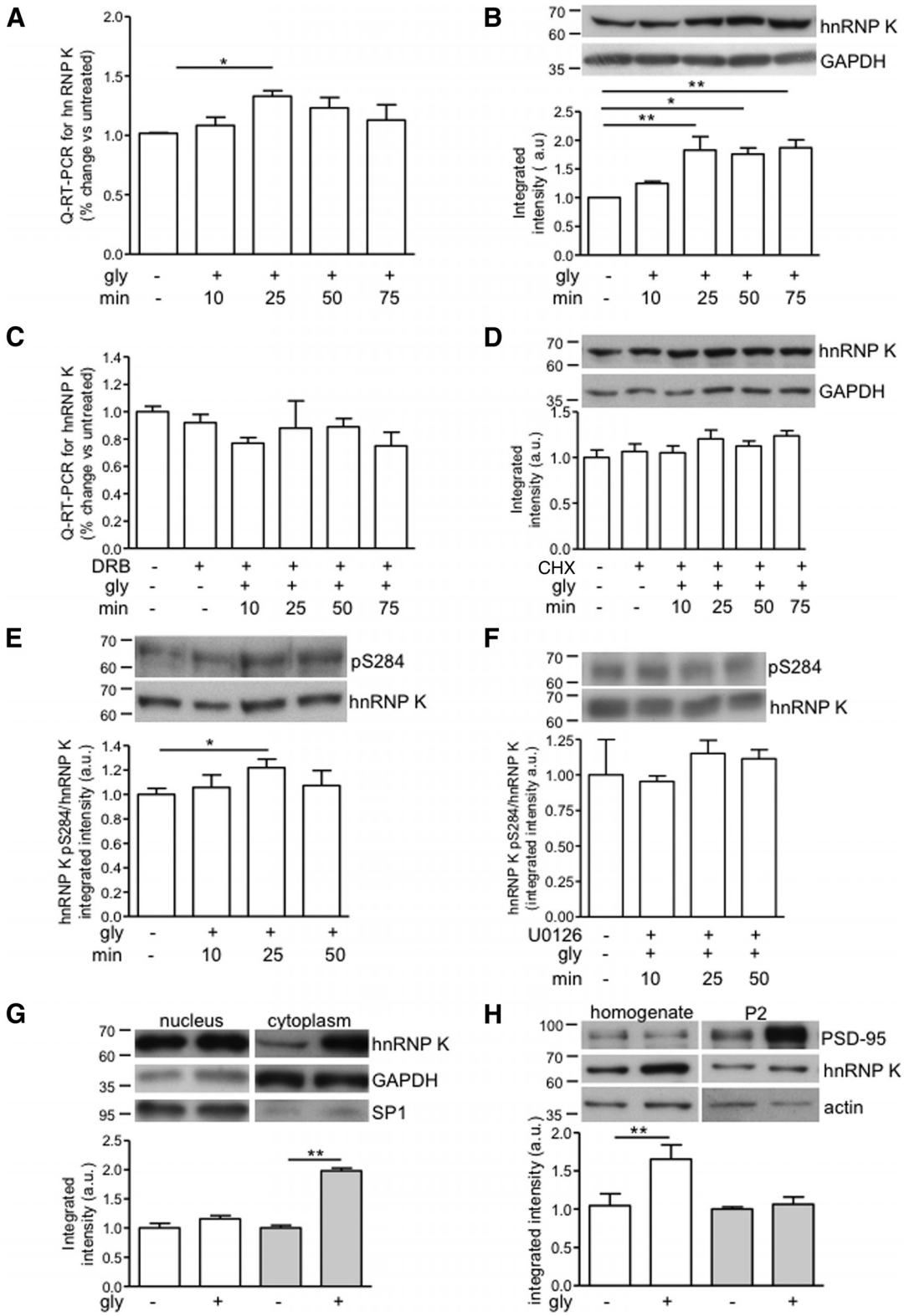

Figure 2. hnRNP K expression and S284 phosphorylation are modulated by cLTP. ***A***, Real-time PCR analysis showing an increase in hnRNP K mRNA levels in neurons after cLTP ($t_{(0)} = 1.01 \pm 0.001$, $p > 0.05$; $t_{(10)} = 1.08 \pm 0.06$, $p > 0.05$; $t_{(25)} = 1.33 \pm 0.04$, $^{*}p < 0.05$; $t_{(50)} = 1.23 \pm 0.08$, $p > 0.05$; $t_{(75)} = 1.12 \pm 0.12$, $p > 0.05$; ANOVA and Dunnett's *post hoc* test; values were normalized against GAPDH). ***B***, Representative WB showing the hnRNP K protein level in the lysates of neurons after LTP induction ($t_{(0)} = 1$; $t_{(10)} = 1.25 \pm 0.04$, $p > 0.05$; $t_{(25)} = 1.83 \pm 0.23$, $^{**}p < 0.01$; $t_{(50)} = 1.76 \pm 0.1$, $^{*}p < 0.05$; $t_{(75)} = 1.87 \pm 0.14$, $^{**}p < 0.01$; ANOVA and Dunnett's *post hoc* test; values were normalized against GAPDH). ***C***, Real-time PCR analysis demonstrating that DRB treatment prevents the increase in hnRNP K mRNA induced by cLTP. ***D***, Representative WB showing that CHX treatment prevents the increase in the hnRNP K protein during cLTP. ***E***, Representative WB showing that cLTP induces hnRNP K phosphorylation of S284 ($t_{(0)} = 1 \pm 0.05$; $t_{(10)} = 1.05 \pm 0.1$, $p > 0.05$; $t_{(25)} = 1.22 \pm 0.07$, $^{*}p < 0.05$; $t_{(50)} = 1.07 \pm 0.12$, $p > 0.05$; values were normalized against total hnRNP K; Student's *t* test). ***F***, Representative WB showing that U0126 treatment prevents the phosphorylation of S284 induced by cLTP. ***G***, ***H***, Subcellular fractionation performed in cLTP-induced neurons revealed an increase in hnRNP K protein in the cytoplasm (1.981 ± 0.048 treated vs 1 ± 0.045 untreated, Student's *t* test $^{**}p < 0.01$) but not in the nucleus or the P2 fraction. GAPDH, SP1, and PSD-95 were used to verify the fraction purity. Gly, glycine.

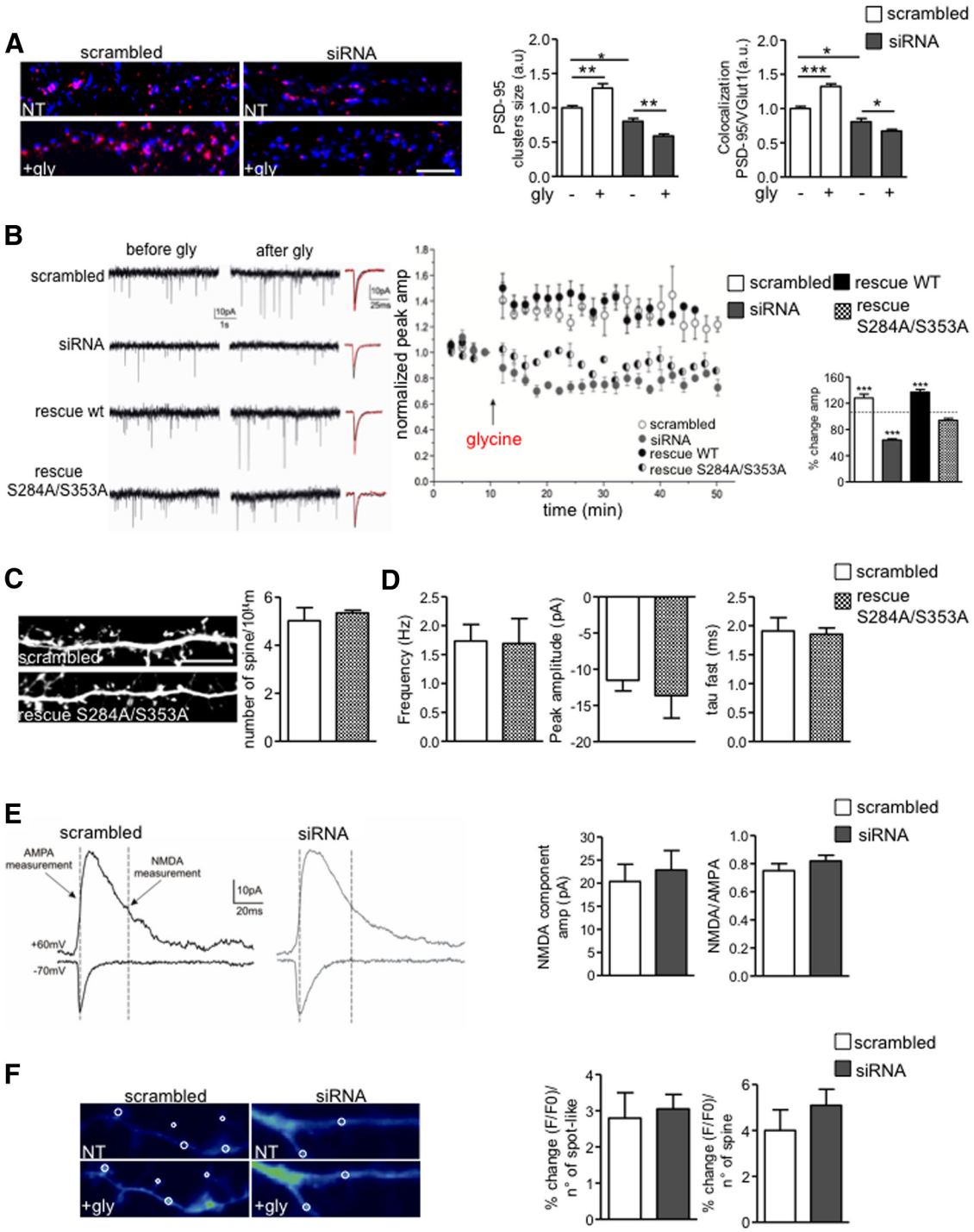

Figure 3. cLTP is impaired in hnRNP K-silenced neurons. ***A***, Infected neurons treated with glycine (gly) were stained for PSD-95 (red) and VGLUT1 (blue) 40 min after treatment. cLTP induced an increase in the PSD-95 cluster size (1.28 ± 0.06 a.u. neurons treated with glycine vs 1 ± 0.03 untreated neurons, Student's *t* test $^{**}p < 0.01$) and PSD-95/VGLUT1 colocalization (1.32 ± 0.04 a.u. neurons treated with glycine vs 1 ± 0.03 untreated neurons; Student's *t* test $^{***}p < 0.001$) in control neurons and a decrease in siRNA neurons (PSD-95 size: 0.8 ± 0.04 vs 0.58 ± 0.03, $^{**}p < 0.01$; PSD-95/VGLUT1: 0.8 ± 0.04 vs 0.67 ± 0.02, $^{***}p < 0.001$). The panels show a merge of the channels under distinct conditions. ***B***, Left, neurons were transfected with scrambled, siRNA, siRNA plus hnRNP K WT (rescue WT), or siRNA plus hnRNP K S284A/S353A (rescue S284A/S353A). Each row shows recordings before and after glycine treatment and the averages of 50 mEPSCs recorded before (black) and after (red) glycine treatment. Right, The average time course is shown. The graph indicates the percentage of amplitude change 5 min after induction (scrambled +28 ± 6%; siRNA −36 ± 2%; rescue WT +37 ± 4%; rescue S284A/S353A −6 ± 3%; $^{***}p < 0.001$). ***C***, Dendritic spine density was analyzed in neurons transfected with scrambled or rescue S284A/S353A ($p > 0.05$). Scale bar, 10 μm. ***D***, Histograms showing the mean mEPSC frequency, peak, amplitude, and decay kinetics for neurons transfected with scrambled or rescue S284A/S353A ($p > 0.05$). ***E***, Average of 50 mEPSCs, showing traces recorded at +60 mV and −70 mV, to compare the NMDA and AMPA components, respectively, of the glutamatergic current. The dashed lines and arrows indicate the point of measurement of the AMPA and NMDA peaks at +60 mV. No differences were detected in the NMDA peak and combined NMDA/AMPA current between neurons transfected with scrambled or siRNA. ***F***, Calcium imaging before and during glycine treatment of neurons transfected with scrambled or siRNA. Histograms represent the average percentage change in the fluorescence normalized against the number of spines, which was estimated by imaging experiments (left) or by morphological analysis (right). NT, not treated.

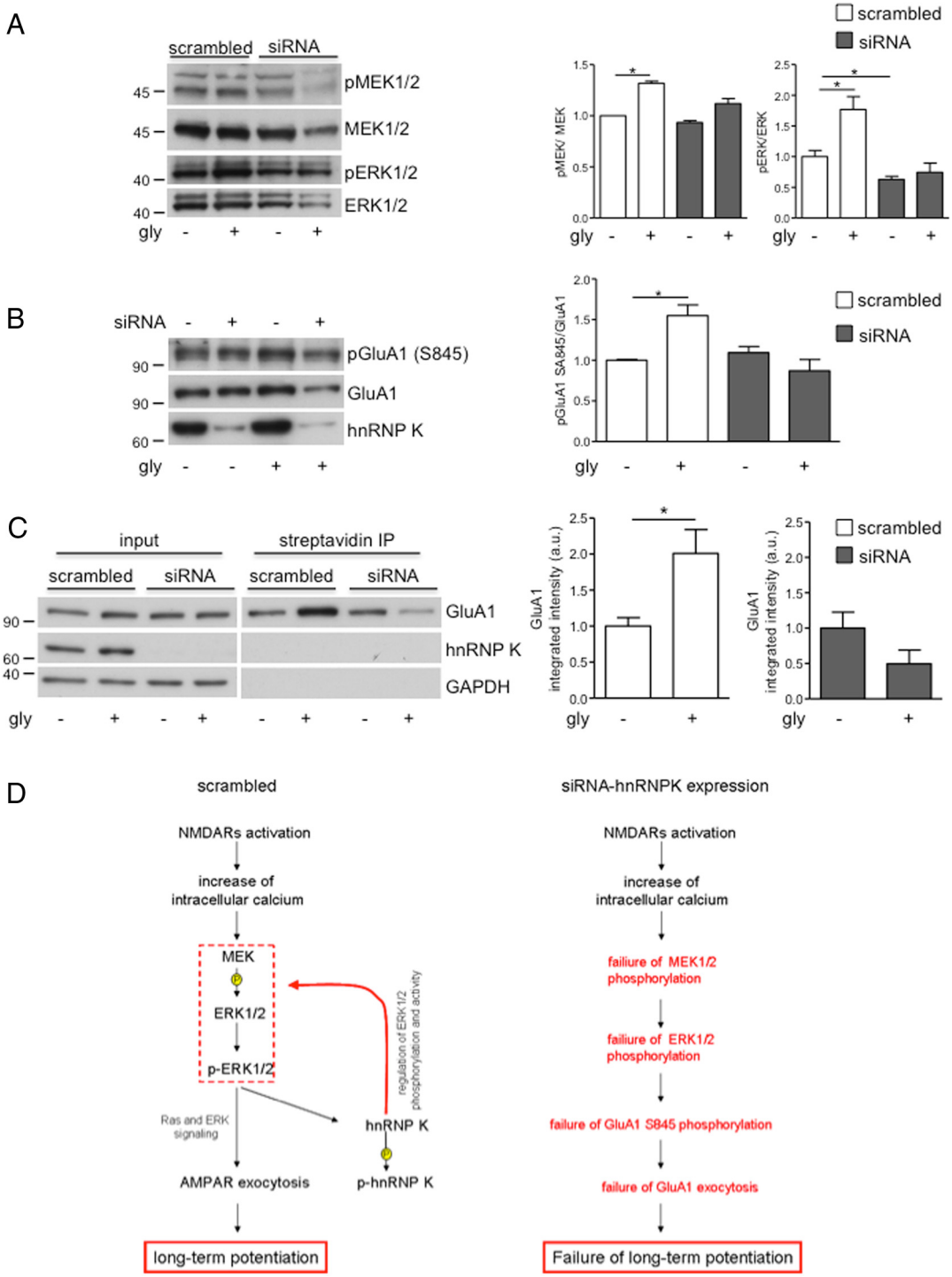

Figure 4. ***A***, ***B***, Representative WB showing the lysates of neurons infected with scrambled or siRNA in the untreated condition and 20 min after cLTP. cLTP increased pMEK, pERK1/2, and pGluA1-S845 in the scrambled neurons (pMEK: 1 ± 0.01 vs 1.31 ± 0.02, Student's *t* test **p* < 0.05; pERK1/2: 1 ± 0.1 vs 1.76 ± 0.2, Student's *t* test **p* < 0.05; S845 pGluA1-S845: 1 ± 0.01 vs 1.54 ± 0.13, Student's *t* test **p* < 0.05) but not in the siRNA neurons (pMEK: 0.93 ± 0.02 vs 1.1 ± 0.05, Student's *t* test *p* > 0.05; pERK1/2: 0.63 ± 0.05 vs 0.74 ± 0.15, Student's *t* test *p* > 0.05; pGluA1-S845: 1 ± 0.02 vs 1.21 ± 0.13, Student's *t* test *p* > 0.05). ***C***, Representative WB showing the surface biotinylation assay probed with an antibody against GluA1 in neurons infected with scrambled or siRNA. cLTP increased GluA1 surface levels only in scrambled neurons (scrambled: 1 ± 0.01 vs 1.55 ± 0.13, Student's *t* test **p* < 0.05; siRNA 1.01 ± 0.07 vs 0.87 ± 0.14, Student's *t* test *p* > 0.05). ***D***, Schematic diagram of the proposed cross talk between hnRNP K and ERK1/2. In the control condition, cLTP induction causes an increase in [Ca2+]i through NMDARs and leads to the activation of the ERK cascade. ERK1/2 activation induces hnRNP K phosphorylation and AMPAR exocytosis, which are required for LTP. In turn, hnRNP K regulates the extent of ERK activation, suggesting positive feedback between hnRNP K and ERK1/2. Upon hnRNP K knockdown, ERK1/2 cascade activation is impaired, both GluA1 phosphorylation on S845 and surface accumulation are prevented, and LTP fails. Gly, glycine.

hnRNP K knockdown inhibits ERK cascade activation and GluA1 membrane delivery during cLTP

Because hnRNP K regulates ERK cascade activation (Mikula and Bomsztyk, 2011), we investigated whether hnRNP K silencing affects ERK1/2 signaling during cLTP. Notably, following cLTP induction, phosphorylated MEK1/2 (pMEK) and ERK1/2 (pERK1/2) increased in scrambled but not siRNA-expressing neurons (Fig. 4*A*).

In neurons, ERK1/2 phosphorylation is required for GluA1 phosphorylation of S845 (pGluA1-S845; Song et al., 2013) and the delivery of GluA1-containing AMPARs to synapses during LTP (Zhu et al., 2002). Accordingly, hnRNP K-silenced neurons did not exhibit an increase in pGluA1-S845 or GluA1 surface expression during cLTP (Fig. 4*B*,*C*).

These data suggest that hnRNP K acts upstream of the ERK1/2 cascade and controls the S845 phosphorylation and surface expression of GluA1 during LTP in hippocampal neurons.

Discussion

This study identified hnRNP K as a key determinant of synapse plasticity in the hippocampus.

hnRNP K colocalizes with dendritic spine markers, and this evidence prompted us to hypothesize a role for hnRNP K in synapse function.

We demonstrated that both the dendritic spine density and mEPSC frequency are reduced in hnRNP K-silenced neurons. Because we recorded hnRNP K-silenced cells that received inputs from untransfected cells, the reduction in the mEPSC frequency likely reflects the lower spine density. Furthermore, the lack of alterations in the mEPSC variation coefficient and in presynaptic marker expression excludes a deficit in presynaptic release. Because the dendritic spine size and mEPSC amplitude do not differ from those of control neurons, the major effect of hnRNP K knockdown is the reduction of dendritic spines, consistent with previous results, demonstrating that hnRNP K knockdown reduces the synapse number in neurons (Proepper et al., 2011).

Hence, our results support a role of hnRNP K in the modulation of synaptogenesis or spine stabilization, thereby controlling the overall dendritic spine density. Because the involvement of hnRNP K in N-WASP and Arp2/3 complex regulation is well established (Yoo et al., 2006; Liu et al., 2008; Proepper et al., 2011), spine defects in silenced neurons are likely the result of the loss of the regulation of cytoskeletal dynamics by hnRNP K. However, the precise mechanisms by which hnRNP K modulates the polymerization of cytoskeleton filaments remain poorly understood. hnRNP K knockdown in mature hippocampal neurons causes an enlargement of the dendritic tree (Proepper et al., 2011), and we observed that hnRNP K knockdown at earlier developmental stages (12 DIV) reduces the dendritic length and branching. Based on these findings, an intriguing hypothesis that warrants closer examination is that the role of hnRNP K in dendritic arborization is developmentally regulated, such that hnRNP K promotes arborization in young neurons while inhibiting it in mature neurons.

Furthermore, hnRNP K-silenced neurons exhibit a reduction in PSD-95 and GluA2 expression levels and in mEPSC decay kinetics compared with control neurons. In addition to reflecting a general reduction in spine number, these data suggest that the GluA2 content at synapses is also reduced; in fact, changes in the subunit composition of AMPAR at the synapse, with a prevalence of GluA1 homomers compared with GluA1-GluA2 heteromers, is generally responsible for the slower mEPSC decay kinetics (Jonas, 2000; Lu et al., 2009).

As cytoskeletal dynamics, together with AMPAR content and subunit composition, are critical determinants of synaptic strength and plasticity (Schwechter and Tolias, 2013), we investigated the potential role for hnRNP K in LTP. Interestingly, we determined that cLTP induction requires both hnRNP K-mediated activation of the ERK cascade and hnRNP K phosphorylation by ERK1/2. The capability of hnRNP K and ERK1/2 for reciprocal activation has been described previously (Mikula and Bomsztyk, 2011), and we investigated the role of this cross talk in LTP.

hnRNP K phosphorylation by ERK1/2 has been reported to enhance hnRNP K nuclear export (Habelhah et al., 2001), consistent with hnRNP K cytoplasmic accumulation after cLTP induction. Furthermore, the capability of hnRNP K to bind ERK1/2 (Laury-Kleintop et al., 2005) prompted us to speculate that hnRNP K could recruit ERK1/2 in the cytoplasm. In addition to its nuclear role, ERK1/2 also plays a postsynaptic role in LTP (Winder et al., 1999). ERK1/2 is required for PKA-mediated phosphorylation of GluA1 at S845 and AMPAR insertion at synapses (Zhu et al., 2002; Song et al., 2013). Notably, hnRNP K silencing precludes GluA1 S845 phosphorylation and surface accumulation during cLTP, which suggests that ERK1/2 and hnRNP K contribute to the regulation of AMPAR trafficking during LTP.

Interestingly, hnRNP K knockdown not only prevented LTP and PSD-95 cluster enlargement but also reduced the mEPSC and PSD-95 cluster area. This result suggests that the loss of hnRNP K function shifted the LTP cascade toward a form of LTD. ERK cascade activation in the hippocampus critically contributes to both LTP and NMDAR-dependent LTD and likely depends on the magnitude and kinetics of ERK activation and its subcellular distribution (Thiels et al., 2002). In particular, it has been proposed that the extent of ERK activation is attenuated in LTD relative to LTP (Thiels et al., 2002). Based on the cross talk between hnRNP K and ERK1/2, we hypothesize that hnRNP K silencing favors LTD induction over LTP by affecting the ERK1/2 activation state.

Although the role of hnRNP K in LTP relies on its ERK-mediated phosphorylation, hnRNP K regulates spine density and basal synaptic transmission regardless of its activation state. Indeed, hnRNP K S284A/S353A was able to rescue spine and mEPSC deficits associated with hnRNP K siRNA expression.

In conclusion, the present study sheds light on a new and unexpected role of hnRNP K in the regulation of dendritic spines and synaptic plasticity in hippocampal neurons and highlights a positive feedback mechanism between hnRNP K and ERK1/2 that is crucial for LTP induction.

References

Bassani S, Cingolani LA, Valnegri P, Folci A, Zapata J, Gianfelice A, Sala C, Goda Y, Passafaro M (2012) The X-linked intellectual disability protein TSPAN7 regulates excitatory synapse development and AMPAR trafficking. Neuron 73:1143–1158. CrossRef Medline

Cummings JA, Mulkey RM, Nicoll RA, Malenka RC (1996) Ca2+ signaling requirements for long-term depression in the hippocampus. Neuron 16:825–833. CrossRef Medline

Ehlers MD (2000) Reinsertion or degradation of AMPA receptors determined by activity-dependent endocytic sorting. Neuron 28:511–525. CrossRef Medline

Gall D, Prestori F, Sola E, D'Errico A, Roussel C, Forti L, Rossi P, D'Angelo E (2005) Intracellular calcium regulation by burst discharge determines bidirectional long-term synaptic plasticity at the cerebellum input stage. J Neurosci 25:4813–4822. CrossRef Medline

Glisovic T, Bachorik JL, Yong J, Dreyfuss G (2008) RNA-binding proteins and post-transcriptional gene regulation. FEBS Lett 582:1977–1986. CrossRef Medline

Habelhah H, Shah K, Huang L, Ostareck-Lederer A, Burlingame AL, Shokat KM, Hentze MW, Ronai Z (2001) ERK phosphorylation drives cytoplasmic accumulation of hnRNP-K and inhibition of mRNA translation. Nat Cell Biol 3:325–330. CrossRef Medline

Jonas P (2000) The time course of signaling at central glutamatergic synapses. News Physiol Sci 15:83–89. Medline

Kim MJ, Futai K, Jo J, Hayashi Y, Cho K, Sheng M (2007) Synaptic accumulation of PSD-95 and synaptic function regulated by phosphorylation of serine-295 of PSD-95. Neuron 56:488–502. CrossRef Medline

Laury-Kleintop LD, Tresini M, Hammond O (2005) Compartmentalization of hnRNP-K during cell cycle progression and its interaction with calponin in the cytoplasm. J Cell Biochem 95:1042–1056. CrossRef Medline

Liu Y, Szaro BG (2011) hnRNP K post-transcriptionally co-regulates multiple cytoskeletal genes needed for axonogenesis. Development 138:3079–3090. CrossRef Medline

Liu Y, Gervasi C, Szaro BG (2008) A crucial role for hnRNP K in axon development in Xenopus laevis. Development 135:3125–3135. CrossRef Medline

Lu W, Man H, Ju W, Trimble WS, MacDonald JF, Wang YT (2001) Activation of synaptic NMDA receptors induces membrane insertion of new AMPA receptors and LTP in cultured hippocampal neurons. Neuron 29:243–254. CrossRef Medline

Lu W, Shi Y, Jackson AC, Bjorgan K, During MJ, Sprengel R, Seeburg PH, Nicoll RA (2009) Subunit composition of synaptic AMPA receptors revealed by a single-cell genetic approach. Neuron 62:254–268. CrossRef Medline

Lynch M, Chen L, Ravitz MJ, Mehtani S, Korenblat K, Pazin MJ, Schmidt EV (2005) hnRNP K binds a core polypyrimidine element in the eukaryotic translation initiation factor 4E (eIF4E) promoter, and its regulation of eIF4E contributes to neoplastic transformation. Mol Cell Biol 25:6436–6453. CrossRef Medline

Mikula M, Bomsztyk K (2011) Direct recruitment of ERK cascade components to inducible genes is regulated by heterogeneous nuclear ribonucleoprotein (hnRNP) K. J Biol Chem 286:9763–9775. CrossRef Medline

Proepper C, Steinestel K, Schmeisser MJ, Heinrich J, Steinestel J, Bockmann J, Liebau S, Boeckers TM (2011) Heterogeneous nuclear ribonucleoprotein k interacts with Abi-1 at postsynaptic sites and modulates dendritic spine morphology. PLoS One 6:e27045. CrossRef Medline

Schwechter B, Tolias KF (2013) Cytoskeletal mechanisms for synaptic potentiation. Commun Integr Biol 6:e27343. CrossRef Medline

Song RS, Massenburg B, Wenderski W, Jayaraman V, Thompson L, Neves SR (2013) ERK regulation of phosphodiesterase 4 enhances dopamine-stimulated AMPA receptor membrane insertion. Proc Natl Acad Sci U S A 110:15437–15442. CrossRef Medline

Thiels E, Kanterewicz BI, Norman ED, Trzaskos JM, Klann E (2002) Long-term depression in the adult hippocampus in vivo involves activation of extracellular signal-regulated kinase and phosphorylation of Elk-1. J Neurosci 22:2054–2062. Medline

Winder DG, Martin KC, Muzzio IA, Rohrer D, Chruscinski A, Kobilka B, Kandel ER (1999) ERK plays a regulatory role in induction of LTP by theta frequency stimulation and its modulation by beta-adrenergic receptors. Neuron 24:715–726. CrossRef Medline

Yoo Y, Wu X, Egile C, Li R, Guan JL (2006) Interaction of N-WASP with hnRNPK and its role in filopodia formation and cell spreading. J Biol Chem 281:15352–15360. CrossRef Medline

Zhang G, Neubert TA, Jordan BA (2012) RNA binding proteins accumulate at the postsynaptic density with synaptic activity. J Neurosci 32:599–609. CrossRef Medline

Zhu JJ, Qin Y, Zhao M, Van Aelst L, Malinow R (2002) Ras and Rap control AMPA receptor trafficking during synaptic plasticity. Cell 110:443–455. CrossRef Medline